The Journal of Neuroscience, October 15, 1999, *19*(20):8839–8848

The *weaver* Mouse *gain-of-function* Phenotype of Dopaminergic Midbrain Neurons Is Determined by Coactivation of *wv*Girk2 and K-ATP Channels

Birgit Liss, Axel Neu, and Jochen Roeper

Medical Research Council, Anatomical Neuropharmacology Unit, Department of Pharmacology, Oxford University and Institute for Neural Signaltransduction, Center for Molecular Neurobiology 20246, Hamburg, Germany

The phenotype of substantia nigra (SN) neurons in homozygous *weaver* (*wv/wv*) mice was studied by combining patch-clamp and single-cell RT-multiplex PCR techniques in midbrain slices of 14-d-old mice. In contrast to GABAergic SN neurons, which were unaffected in homozygous *weaver* mice (*wv/wv*), dopaminergic SN neurons possessed a dramatically altered phenotype with a depolarized membrane potential and complete loss of spontaneous pacemaker activity. The *gain-of-function* phenotype was mediated by a large, nonselective membrane conductance exclusively present in (*wv/wv*) dopaminergic SN neurons. This constitutively activated conductance displayed a sensitivity to external QX-314 (IC_{50} = 10.6 μM) very similar to that of heterologously expressed *wv*Girk2 channels and was not further activated by G-protein stimulation. Single-cell Girk1–4 expression profiling suggested that homomeric Girk2 channels were present in most dopaminergic SN neurons, whereas Girk2 was always coexpressed with other Girk family members in GABAergic SN neurons. Surprisingly, acute QX-314 inhibition of *wv*Girk2 channels did not induce wild-type-like pacemaker activity but instead caused membrane hyperpolarization. Additional application of a blocker of ATP-sensitive potassium channels (100 μM tolbutamide) induced wild-type-like pacemaker activity. We conclude that the *gain-of-function weaver* phenotype of dopaminergic substantia nigra neurons is mediated by coactivation of *wv*Girk2 and SUR1/Kir6.2-mediated ATP-sensitive K^+ channels. We also show that in contrast to wild-type neurons, all (*wv/wv*) dopaminergic SN neurons expressed calbindin, a calcium-binding protein that marks dopaminergic SN neurons resistant to neurodegeneration. The identification of two ion channels that in concert determine the *weaver* phenotype of surviving calbindin-positive dopaminergic SN neurons will help to understand the molecular mechanisms of selective neurodegeneration of dopaminergic SN neurons in the *weaver* mouse and might be important in Parkinson's disease.

Key words: weaver*; dopamine; substantia nigra; Girk2; K-ATP channel; single-cell RT-PCR; neurodegeneration; Parkinson's disease*

The neurological phenotype of the *weaver* mouse (Lane, 1964) consists of the selective degeneration of cerebellar granule cells (Rezai and Yoon, 1972; Rakic and Sidman, 1973) and dopaminergic neurons in the substantia nigra (Schmidt et al., 1982) in homozygous mutants. A missense mutation (G953A) in the Girk2 gene (KCNJ6), which codes for a subunit of a G-protein-activated inwardly rectifiying K^+ channel, was recently identified in the *weaver* mouse (Patil et al., 1995). The mutation results in a single amino acid substitution (G156S) in the GYG-selectivity filter of the Girk2 channel pore. In consequence, heterologously expressed homomeric *wv*Girk2 mediates nonselective cationic channels (Kofuji et al., 1996; Navarro et al., 1996; Slesinger et al., 1996). Recombinant *wv*Girk2 channels were also constitutively active and did not show physiological activation by G-proteins. It is not clear whether heteromerization of *wv*Girk2 with other members of the Girk family (Girk1–4 or Kir3.1–3.4) alters the *gain-of-function wv*Girk2 channel phenotype (Kofuji et al., 1996; Navarro et al., 1996; Slesinger et al., 1996). These studies in heterologous expression systems indicated that the effect of the *weaver* mutation in different neuronal populations might depend on their cell-specific gene expression profiles, in particular, of the Girk-family. Because Girk2 is widely present in many neuronal populations (Liao et al., 1996), differences in coexpression pattern might also explain the high selectivity of neurodegeneration in *weaver* brain, which targets cerebellar granule and dopaminergic midbrain neurons. Interestingly, equivalent pore mutations in other potassium channels either lead to *gain-of-function* (Sh_{G444S}, Heginbotham et al., 1994) or negative dominant, *loss-of-function* phenotypes ($Kir6.2_{G132S}$, Miki et al., 1997; $KCNQ4_{G285S}$, Kubisch et al., 1999).

The generation of a Girk2 knock-out mouse demonstrated that a simple *loss-of-function* was not sufficient to reproduce the selective neurodegeneration found in *weaver* (Signorini et al., 1997). *Loss-of-function* as well as *gain-of-function* phenotypes have been described for cultured *weaver* granule cells (Kofuji et al., 1996; Surmeier et al., 1996; Slesinger et al., 1997). A recent *in vitro* brain slice study on premigratory *weaver* granule cells, which is the developmental stage associated with *weaver*-mediated degeneration, reported a *loss-of-function* of G-protein-activated K^+ channels (Rossi et al., 1998). Thus, the description of the electrophysiological phenotype of *weaver* granule cells remains controversial.

The electrophysiological properties and the neurodegenerative

Received June 18, 1999; revised Aug. 5, 1999; accepted Aug. 10, 1999.

This work was supported by grants of the Deutsche Forschungsgemeinschaft and the Medical Research Council to J.R. B.L. is a Blaschko Visiting Research Scholar at Linacre College, Oxford, UK. J.R. holds the Monsanto Senior Research Fellowship at Exeter College, Oxford, UK .We thank Stefan Freischmidt for excellent care of the *weaver* breeding colony, Oliver Franz for help with graphics, and Frances Ashcroft for discussion.

Correspondence should be addressed to Dr. Jochen Roeper, Medical Research Council Anatomical Neuropharmacology Unit, Oxford University, Mansfield Road, Oxford OX1 3TH, UK.

mechanisms of dopaminergic substantia nigra neurons in the homozygous *weaver* mouse are unknown. Their degeneration is most dramatic in the first three postnatal weeks when already 50% of these neurons die (Bayer et al., 1995a; Verney et al., 1995). Similar to the neurodegenerative pattern of dopaminergic midbrain neurons in Parkinson's disease and its neurotoxicological animal models, dopaminergic subpopulations are differentially affected in the *weaver* mouse (Graybiel et al., 1990), and a calbindin-positive subpopulation of DA neurons survives (Gaspar et al., 1994). In addition, late-generated dopaminergic SN neurons preferentially die in the *weaver* mouse (Bayer et al., 1996). Because similar subpopulations of vulnerable dopaminergic SN neurons are targeted in *weaver* and in Parkinson's disease, it is possible that the sequences of cellular events leading to selective neurodegeneration converge at a point downstream of an initial trigger mechanism. In *weaver*, the Girk2 mutation sets a well defined starting point, whereas for Parkinson's disease a similar Girk2 mutation has been excluded, and the etiology is still unknown (Bandmann et al., 1996). Thus, understanding the phenotype of (*wv*/*wv*) dopaminergic SN neurons might have important implications beyond this particular mouse model. To analyze the cellular phenotype of dopaminergic SN neurons during the period of massive neurodegeneration, we combined whole-cell patch-clamp and single-cell RT-multiplex PCR (RT-mPCR) techniques in acute midbrain slices of 14-d-old postnatal *weaver* and control mice.

MATERIALS AND METHODS

Slice preparation. Unaffected (+/+), heterozygous (wv/+), and homozygous (wv/wv) *weaver* mutant mice (B6CBACa-A^{w-J}/A-wv) and C57Bl/6J mice were used (14 postnatal days old). Homozygous *weaver* mice were obtained by intercross mating of heterozygous *weaver* mice (The Jackson Laboratory, Bar Harbor, ME). Genotypes were defined by DNA analysis from tail biopsies. Mice were deeply anesthetized with halothane and then decapitated. Brains were removed quickly, immersed in ice-cold solution, and then blocked for slicing. Thin coronal midbrain slices (250 μm) were cut with a Vibroslice (Campden Instruments, London, UK) while bathed in an ice-cold artificial CSF (ACSF) containing (in mM): 125 NaCl, 25 $NaHCO_3$, 2.5 KCl, 1.25 NaH_2PO_4, 2 $CaCl_2$, 2 $MgCl_2$, and 25 glucose, bubbled with a mixture of 95% O_2 and 5%CO_2. After sectioning, midbrain slices were maintained submerged in a holding chamber filled with gassed ACSF and allowed to recover >30 min at room temperature (22–24°C) before the experiment. Midbrain slices containing a clearly defined substantia nigra pars compacta at the level of the rostral interpeduncularis nucleus and the caudal mammillary nucleus (corresponding to levels 2 and 3; Nelson et al., 1996) were used for the experiments.

Whole-cell recordings and data analysis. For patch-clamp recordings, midbrain slices were transferred to a chamber continuously perfused at 2–4 ml/min with ACSF bubbled with a mixture of 95% O_2 and 5% CO_2 at room temperature (22–24°C). Patch pipettes (1–2.5 MΩ) pulled from borosilicate glass (GC150TF; Clark, Reading, UK) were filled with internal solution containing (in mM): 120 K-gluconate, 20 KCl, 10 HEPES, 10 EGTA, 2 $MgCl_2$, and 2 Na_2ATP, pH 7.3 (290–300 mOsm). Whole-cell recordings were made from neurons visualized by infrared differential interference contrast videomicroscopy with a Newvicon camera (C2400; Hamamatsu, Hamamatsu City, Japan) mounted to an upright microscope (Axioskop FS; Zeiss, Oberkochen, Germany) (Stuart et al., 1993). Recordings were performed in current-clamp and voltage-clamp mode using an EPC-9 patch-clamp amplifier (Heka Elektronik, Lambrecht, Germany). Only experiments with uncompensated series resistances <10 MΩ were included in the study, and series resistances were electronically compensated (50–75%). The program package Pulse + Pulsefit (Heka) was used for data acquisition and analysis. Leakage and capacitive currents were subtracted on-line using the P/4 subtraction method as indicated. Records were digitized at 2–5 kHz and filtered with low-pass filter Bessel characteristic of 1 kHz cutoff frequency. DMSO- or NaOH-stock solutions of the drugs were diluted 1000-fold in an external solution containing (in mM): 145 NaCl, 2.5 KCl, 10 HEPES, 2 $CaCl_2$, 2 $MgCl_2$, and 25 glucose, pH 7.4, and applied locally under visual control using a buffer pipette attached to a second manipulator. Switching between control and drug-containing solutions was controlled by an automated application system (AutoMate Scientific, Oakland, CA). Data were given as mean ± SEM. To evaluate statistical significance, data were subjected to Student's *t* test in Sigmaplot (Jandel Scientific, San Rafael, CA).

Cytoplasm harvest and RT. For single-cell RT-PCR experiments, the patch pipettes were filled with 6 μl of autoclaved internal RT-PCR solution containing (in mM): 140 KCl, 5 HEPES, 5 EGTA, and 3 $MgCl_2$, pH 7.3. At the end of the recording (<15 min), the cell contents (including the nucleus, in most cases) were aspirated as complete as possible into the patch pipette under visual control (40× objective and 2–4 × zoom) by application of gentle negative pressure. Cells were only further analyzed when the whole-cell configuration remained stable throughout the harvesting procedure. Pipettes were then quickly removed from the cell, washed two times through the solution interface, and the pipette contents were immediately expelled into a 0.5 ml test tube containing the contents for reverse transcription. First strand cDNA was synthesized for 1 hr at 37°C in a total reaction volume of 10 μl containing random hexamer primers (Boehringer Mannheim, Indianapolis, IN; final concentration, 5 μM), dithiothreitol (final concentration, 10 mM), the four deoxyribonucleotide triphosphates (Pharmacia, Piscataway, NJ; final concentration, 0.5 mM each), 20 U of ribonuclease inhibitor (Promega, Madison, WI) and 100 U of reverse transcriptase (Superscript II; Life Technologies, Gaithersburg, MD). The single-cell cDNA was kept at −70°C until PCR amplification.

Multiplex and nested PCR. After reverse transcription, the cDNAs for Girk1, Girk2, Girk3, and Girk4, TH, and GAD67 or SUR1, SUR2, Kir6.2, Kir6.1, calbindin D_{28K}, TH, and GAD67 were simultaneously amplified in a multiplex PCR using the following set of primers (from 5′ to 3′). Primer pairs for TH, GAD67, SUR1, SUR2, Kir6.2, Kir6.1 were identical to those used in Liss et al. (1999): Girk1 (accession number D45022) sense, AGACCAGTCGCTACCTTTCG (position 233), antisense, TCCTGCTCT TTCACGCTGTA (position 1130); Girk2 (accession number U11859) sense, CCTACCGATACCTGACGGAC (position 711), antisense, GGGTGCTGG TCTCATAGGTC (position 1580); Girk3 (accession number U11860) sense, TCACTTGGCTCTTCTTCGGT (position 556), antisense, GTAGAGATGG GCATCAAGGC (position 1357); Girk4 (accession number U33631) sense, GTGTTGAAAACCTTAGCGGC (position 386), antisense, CACCCTCTTC ATCCTTCTCG (position 1213); and calbindin (accession number M21531) sense, CGCACTCTCAAACTAGCCG (position 87), antisense, CAGCCTACTTC TTTATAGCGCA (position 977). First multiplex PCR was performed as hot start in a final volume of 100 μl containing the 10 μl reverse transcription reaction, 100 pmol of each primer, 0.2 mM each dNTP (Pharmacia), 1.8 mM $MgCl_2$, 50 mM KCl, 20 mM Tris-HCl, pH 8.4, and 3.5 U *Taq*-polymerase (Life Technologies) in a Perkin-Elmer Thermal Cycler 480C with the following cycling protocol: after 3 min at 94°C, 35 cycles (94°C, 30 sec; 58°C, 60 sec; 72°C, 3 min) of PCR were performed followed by a final elongation period of 7 min at 72°C. The nested PCR amplifications were performed in individual reactions, in each case with 2.5 μl of the first PCR reaction product under similar conditions with the following modifications: 50 pmol of each primer, 2.5 U *Taq*-polymerase, 1.5 mM $MgCl_2$, and a shorter extension time (60 sec) using the following primer pairs: Girk1 sense, GACCCTGATGTTTAGCGAGC (position 621), antisense, TGACGACAACCTCGAACTGT (position 937); Girk2 sense, TACATCCGGGGAGATATGGA (position 936), antisense, GAACCCGTC TTCCATCGTTA (position 1531); Girk3 sense, ATGTTCGTCAAGATCTCGCA (position 776), antisense, CATCCACCAGGTACGAGCTT (position 1188); Girk4 sense, CCTTGAACCAGACCGACA (position 752), antisense, CACCCTCTTCATCCTTCTCG (position 1009); and calbindin sense, GAGATCTGGCTTCATTTCGAC (position 167), antisense, AGTTCCAGCTTTCCGTCATTA (position 606). To investigate the presence and size of the amplified fragments, 15 μl aliquots of PCR products were separated and visualized in ethidium bromide-stained agarose gels (2%) by electrophoresis. The predicted sizes (base pairs) of the PCR-generated fragments were: 316 (Girk1), 693 (Girk2), 412 (Girk3), 257 (Girk4), 377 (TH), 702 (GAD67), and 215 (SUR2), 298 (Kir6.2), 401 (SUR1), 448 (Kir6.1), and calbindin (440). All individual PCR products were verified several times ($n > 3$) by direct sequencing or subcloning and sequencing.

RNA isolation and cDNA preparation for control reactions. Poly(A)$^+$ RNA was prepared from ventral midbrain of 13-d-old C57Bl/6J mice

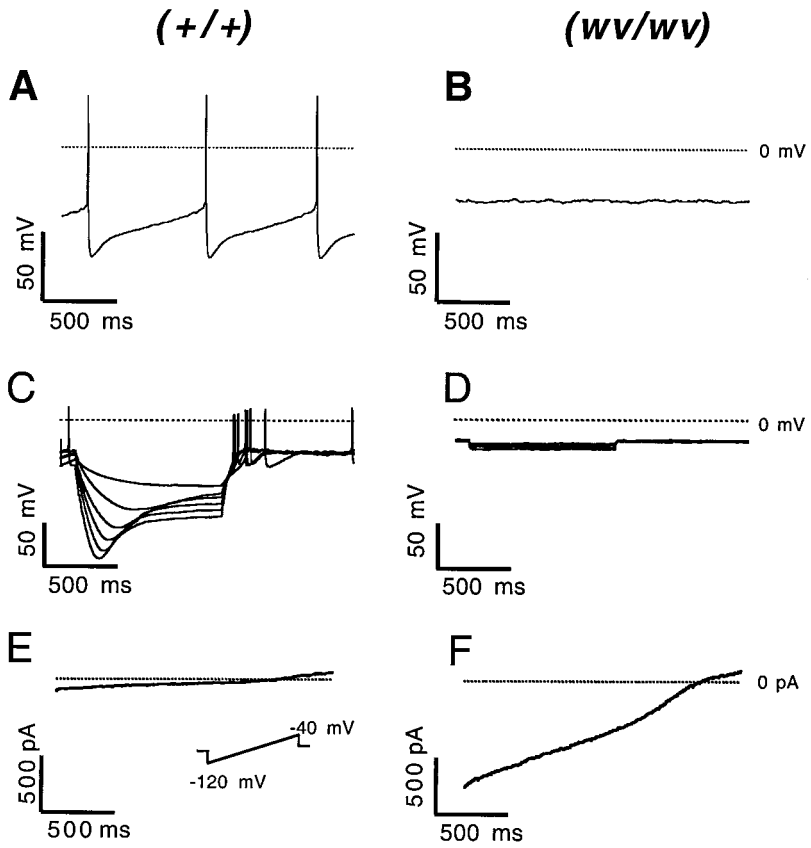

Figure 1. Electrophysiological phenotype of (*wv/wv*) dopaminergic SN neurons. *A*, *B*, Standard whole-cell current-clamp recordings of spontaneous electrical activity in dopaminergic SN neurons of wild-type (+/+) and homozygotic *weaver* (*wv/wv*) mouse. *C*, *D*, Responses of membrane potential to injection of hyperpolarizing currents of increasing amplitudes from −25 to −150 pA in steps of 25 pA in (+/+) and (*wv/wv*) dopaminergic SN neurons. *E, F*, Current response to voltage ramps from −120 to −40 mV from a holding potential of −60 mV in (+/+) and (*wv/wv*) dopaminergic SN neurons. *Dotted lines* indicate zero levels.

using the Micro-FastTrack Kit (Invitrogen, San Diego, CA). The reverse transcription was performed with 500 ng of poly(A)$^+$ RNA as described above. For the positive controls performed in parallel with each single-cell amplification, the resulting midbrain cDNA-stock was diluted 1000-fold, and 1 μl was used as template for the PCR reaction. All PCR fragments were detected routinely in the positive control with the PCR protocol described above. Negative controls were performed in parallel to single-cell experiments excluding only the harvesting procedure and resulted in no detectable bands. To probe for possible amplification of genomic DNA from the harvested single nuclei, single-cell mPCR amplifications were performed without previous reverse transcription. For all analyzed neurons ($n = 8$), no PCR products were detectable. When possible, primer pairs were designed to be intron-spanning.

RESULTS

We analyzed the electrophysiologcal properties of dopaminergic SN neurons in heterozygous (+/*wv*) and homozygous (*wv/wv*) mutant *weaver* mice, as well as in nonaffected littermates (+/+), using the whole-cell patch-clamp technique in midbrain slices from 14-d-old mice. As shown in Figure 1*A*, all (+/+) dopaminergic SN neurons displayed the well-described low frequency pacemaker activity (1.4 ± 0.7 Hz; $n = 15$) with depolarized thresholds (−36.6 ± 0.8 mV; $n = 15$), and broad action potentials (7.5 ± 0.4 mV; $n = 15$) as reported for dopaminergic SN neurons from C57Bl/6J mouse (Liss et al., 1999) and other species (Grace and Onn, 1989; Lacey et al., 1989; Richards et al., 1997). Only 34% of dopaminergic SN neurons from heterozygous (+/*wv*) animals ($n = 29$) showed spontaneous activity with action potential characteristics not significantly different ($p > 0.05$) compared to those of wild-type neurons [1.5 ± 0.4 Hz, $n = 10$, data not shown; AHP (+/+), −58.5 ± 1.3 mV, $n = 15$; AHP (+/*wv*), −53.8 ± 2.5 mV, $n = 10$; AP (+/+), 7.5 ± 0.4 msec, $n = 15$, AP (+/*wv*), 7.0 ± 0.3 msec, $n = 10$]. However, (+/*wv*) dopaminergic SN neurons possessed more depolarized thresholds (−31.4 ± 0.9 mV; $n = 10$; $p < 0.0005$) compared to wild-type. In contrast to these minor differences between dopaminergic SN neurons from heterozygous and unaffected mice, the phenotype of the dopaminergic SN neurons from homozygous *weaver* was dramatically different. None of the analyzed (*wv/wv*) dopaminergic SN neurons was spontaneously active, and all had depolarized membrane potentials (−34.0 ± 1.2 mV; $n = 40$; Fig. 1*B*). Voltage responses to current injections were minimal, indicating a large increase in membrane conductance in (*wv/wv*) dopaminergic SN neurons compared to wild-type (Fig. 1*C,D*). Indeed, current responses to voltage ramps from −120 to −40 mV demonstrated a large increase of resting membrane conductance (*wv/wv,* 8.8 ± 0.6 nS, $n = 40$; +/+, 1.6 ± 0.2 nS, $n = 23$; Fig. 1*E,F*). The resting membrane conductance of dopaminergic (+/*wv*) SN neurons was also significantly elevated (5.2 ± 0.6; $n = 29$) whereas that in unaffected siblings was almost identical to that obtained in C57Bl/6J mouse (Liss et al., 1999). The altered (*wv/wv*) phenotype was specific for the dopaminergic neurons in the substantia nigra. (*wv/wv*) GABAergic SN neurons displayed a pattern of spontaneous activity (9.8 ± 1.7 Hz; $n = 8$) similar to those observed in controls (Liss et al., 1999). In contrast to cerebellar (*wv/wv*) granule cells in brain slices (Rossi et al., 1998), the presence of a dramatically increased membrane conductance in combination with a depolarization block of spontaneous activity clearly indicates a *gain-of-function* phenotype for (*wv/wv*) dopaminergic SN neurons.

Recent studies of heterologously expressed homomeric *wv*Girk2 channels have demonstrated that mutant Girk2 channels possess a high sensitivity to externally applied cation blockers like QX-314 compared to wild-type Girk2. Application of 100 μM QX-314 had no effect on electrical activity of (+/+) dopaminer-

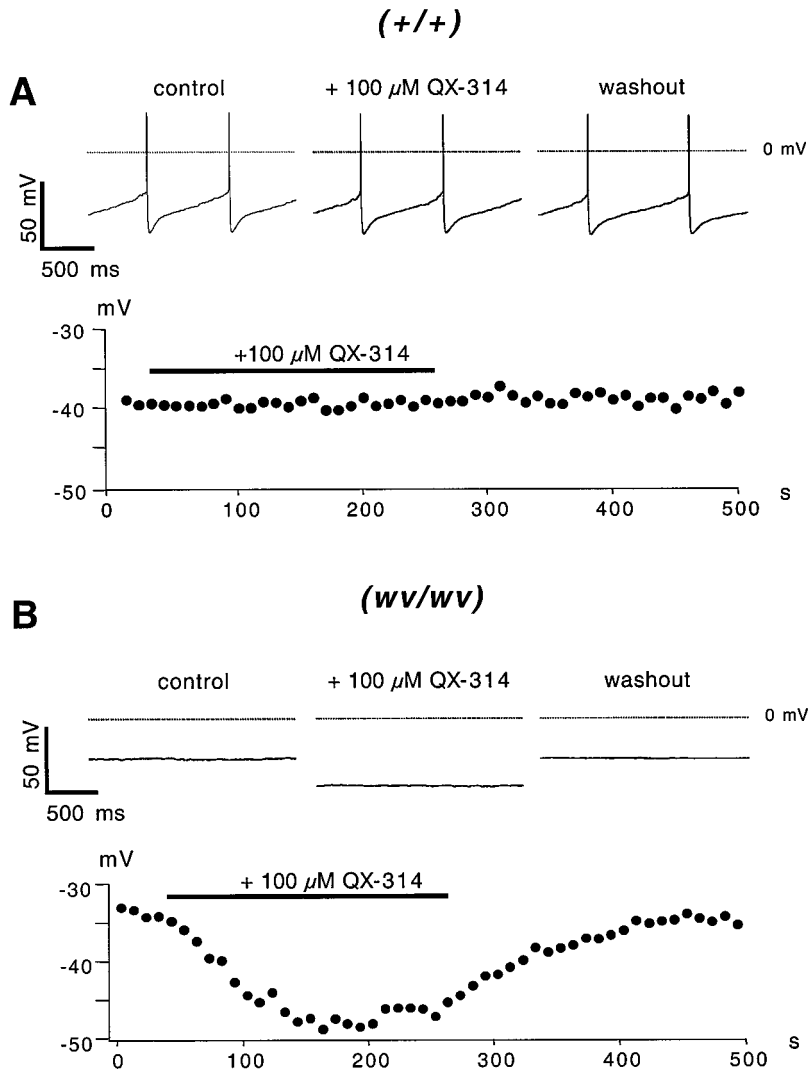

Figure 2. QX-314 selectively affects membrane potential of (*wv/wv*) dopaminergic SN neurons. *A, B*, Standard whole-cell current-clamp recordings of spontaneous electrical activity in wild-type (+/+) and homozygotic weaver (*wv/wv*) dopaminergic SN neurons. *Top panels* show activity under control, in the presence of 100 μM QX-314, and after washout of QX-314. *Bottom panels* plot the membrane potential determined in 10 sec intervals against time. *Dotted lines* indicate zero levels. *Bars* indicate application of QX-314.

gic SN neurons ($n = 6$; Fig. 2*A*) and did not block native membrane conductances present in dopaminergic SN neurons (data not shown). In contrast, 100 μM application of QX-314 induced a reversible membrane hyperpolarization in (*wv/wv*) dopaminergic SN neurons (-51.3 ± 2.7 mV; $n = 14$; Fig. 2*B*). Current responses to voltage ramps from −120 to 0 mV indicated the presence of a constitutively active, linear QX-314-sensitive conductance that had a mean reversal potential of -24.2 ± 3.5 mV ($n = 8$), consistent with the mixed cationic selectivity of Girk2 channels carrying the *weaver* mutation (Kofuji et al., 1996; Navarro et al., 1996; Slesinger et al., 1996) and a mean conductance of 5.7 ± 0.5 nS ($n = 8$; Fig. 3*A,B*). This conductance had an IC_{50} for QX-314 of 10.6 ± 2.0 μM ($n = 6$; Fig. 3*C*), which was very similar to that determined for heterologously expressed *wv*Girk2 channels. To study the G-protein regulation of these channels, we dialyzed wild-type and (*wv/wv*) dopaminergic neurons with 100 μM GTPγS. In wild-type DA neurons, GTPγS activated an inwardly rectifying membrane conductance with a mean reversal potential of -92.7 ± 2.2 mV ($n = 6$; Fig. 4*A,B*) consistent with a highly K^+-selective G-protein-activated conductance previously described in dopaminergic SN neurons (Kim et al., 1995; Lacey et al., 1988; Inanobe et al., 1999). In (*wv/wv*), GTPγS dialysis did not activate or alter subthreshold conductances ($n = 7$; Fig. 4*C*), which is consistent with constitutively active *wv*Girk2 channels with defective G-protein modulation.

The properties of this novel conductance identified in (*wv/wv*) dopaminergic SN neurons strongly suggested that it was mediated by homomeric *wv*Girk2 channels. To directly address this question we designed a single-cell RT-multiplex PCR protocol to determine the mRNA expression profile of the Girk1–4 channel family in SN neurons. RT-PCR experiments demonstrated that all four Girk subunits are expressed in mouse midbrain (Fig. 5*A*). We combined the Girk expression profile with the detection of marker-gene expression to identify SN neurons as either dopaminergic [tyrosine hydroxylase-positive (TH^+) and glutamate decarboxylase-negative (GAD^-)] or GABAergic (TH^-GAD^+) (Liss et al., 1999). Electrophysiological recordings of neurons molecularly characterized by single-cell PCR confirmed that only dopaminergic (TH^+GAD^-) SN neurons possessed the *gain-of-function* phenotype. The majority of dopaminergic SN neurons in wild-type and homozygotic weaver exclusively expressed Girk2 (Figs. 5*B*, 6*A*). In contrast, all analyzed (+/+) and (*wv/wv*) GABAergic SN neurons coexpressed Girk2 with the other Girk family members Girk1 and Girk4 (Figs. 5*C*, 6*B*). Compared to wild-type, the coexpression profiles of (*wv/wv*) dopaminergic SN neurons were not significantly different ($p > 0.05$; Fig. 6*A*). In

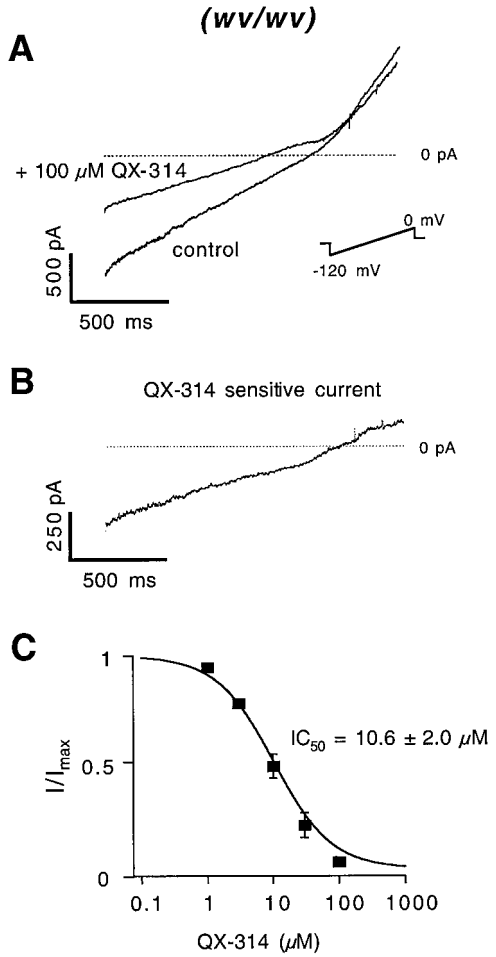

Figure 3. QX-314 blocks a constitutively active conductance in (*wv*/*wv*) dopaminergic SN neurons. *A,* Current responses of a (*wv*/*wv*) dopaminergic SN neuron to voltage ramps from −120 to 0 mV from a holding potential of −60 mV under control conditions and in the presence of 100 μM QX-314 as indicated. *B,* QX-314-sensitive current obtained by subtraction of traces in *A*. *Dotted lines* indicate zero levels. *C,* Dose–response curve for QX-314 inhibition of whole-cell currents in (*wv*/*wv*) dopaminergic SN neurons. *Filled squares* represent means of six separate experiments. *Vertical lines* indicate SEM. Where no lines are apparent, error was smaller than symbol size. The line represents the fit of the mean data by Hill equations with an IC_{50} of 10.6 μM and a Hill coefficient of 1.

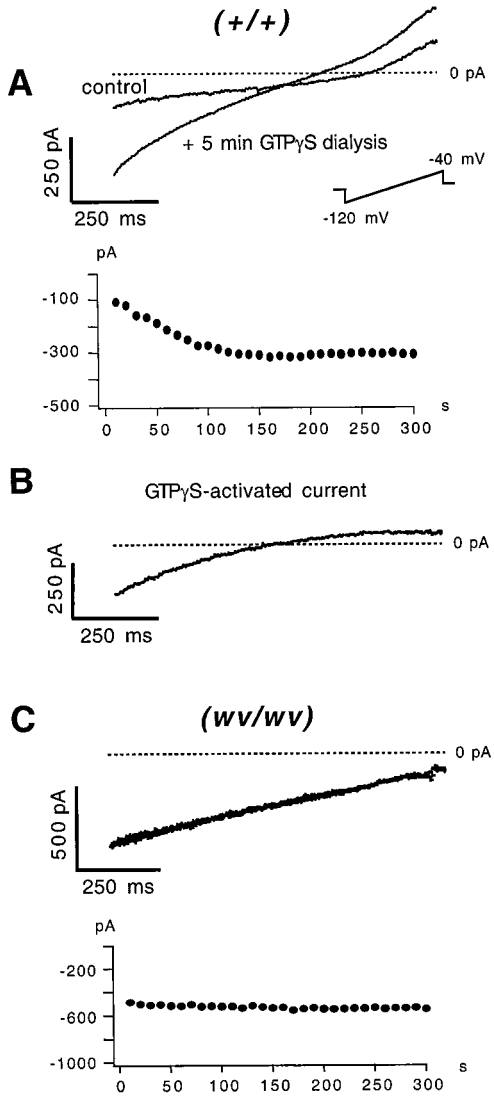

Figure 4. Absence of G-protein activation of Girk channels in (*wv*/*wv*) dopaminergic SN neurons. *A*, *C*, Current responses of a (+/+) and a (*wv*/*wv*) dopaminergic SN neuron to voltage ramps from −120 to −40 mV from a holding potential of −60 mV under control conditions immediately after establishing the whole-cell configuration and after 5 min of dialysis with 100 μM GTPγS as indicated. *Dotted lines* indicate zero levels. *Bottom panels* plot the time course of inward current at −120 mV during GTPγS dialysis. *B,* GTPγS-sensitive current obtained by subtraction of traces in *A*.

addition, dopaminergic (*wv*/*wv*) SN neurons with Girk2 + 1 or Girk2 + 3 coexpression profiles had membrane conductances not significantly different from those expressing only Girk2 (Girk2, 10.4 ± 3.8 nS, $n = 5$; Girk2 + Girk1, 9.8 ± 2.3 nS, $n = 4$; Girk2 + Girk3, 11.8 ± 3.4, $n = 3$). These single-cell PCR experiments suggest that homomeric *wv*Girk2 channels are mainly responsible for the phenotype of dopaminergic SN neurons. However, we found no evidence that the presence of Girk1 or Girk3 mRNA, in addition to that of Girk2, affected the electrophysiological phenotype of (*wv*/*wv*) dopaminergic SN neurons.

Does the tonic activity of nonselective *wv*Girk2 channels fully explain the phenotype of (*wv*/*wv*) dopaminergic SN neurons? If so, acute inhibition of the mutant Girk2 channels by 100 μM QX-314 would be expected to reintroduce wild-type-like electrical behavior in (*wv*/*wv*) dopaminergic SN neurons. Surprisingly, acute application of 100 μM QX-314 did not reestablish pacemaker activity but rather induced a membrane hyperpolarization not accompanied by spontaneous electrical activity. In addition, the resting membrane conductance in the presence of 100 μM QX-314 was still elevated (3.1 ± 0.5 nS; $n = 8$) in (*wv*/*wv*) dopaminergic SN neurons compared to wild-type. This indicated that additional membrane processes were involved in determining the *weaver* phenotype. As the elevated sodium influx via *wv*Girk2 channels was likely to cause metabolic stress (Seutin et al., 1996) we reasoned that secondary activation of ATP-sensitive potassium (K-ATP) channels in DA neurons might be a candidate mechanism for explaining the hyperpolarized state of *weaver* DA neurons after acute application of QX-314. Indeed, application of 100 μM of the sulfonylurea tolbutamide, a K-ATP channel blocker, in the presence of QX-314 repolarized the membrane close to physiological resting membrane potentials (−38.2 ± 2.2 mV; $n = 9$) and induced wild-type-like electrical activity in 67% of *weaver* dopaminergic SN neurons (Fig. 7). The tolbutamide-

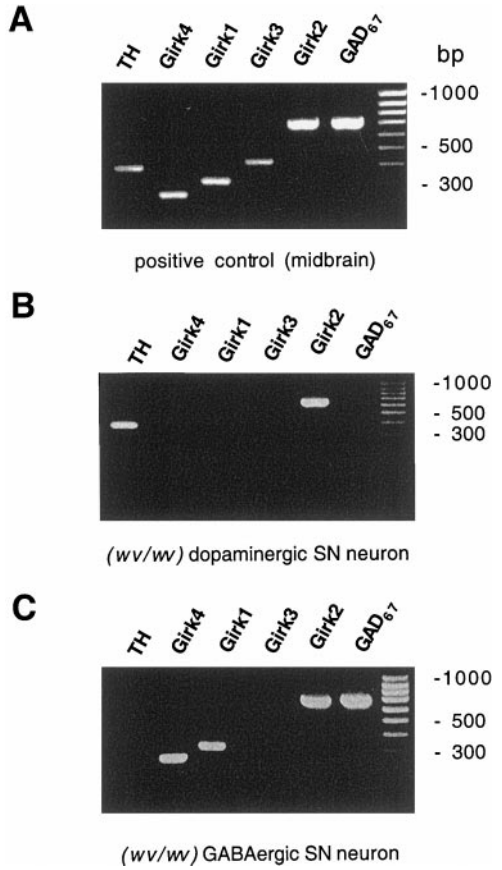

Figure 5. Single-cell RT-multiplex PCR of the Girk channel family in dopaminergic and GABAergic SN neurons. *A,* The six PCR products of nested PCR reactions were resolved in separate lanes by gel electrophoresis in parallel with a 100 bp ladder as molecular weight marker and stained with ethidium bromide. All four Girk channel subunits and the two marker transcripts (TH, GAD67) are expressed in mouse midbrain (positive control). The amplified fragments had the size (in base pairs) predicted by their mRNA sequences, and all fragments were verified by sequencing: TH (377), Girk4 (257), Girk1 (316), Girk3 (412), Girk2 (693), and GAD67 (702). *B,* mPCR expression profiling of a single (*wv/wv*) dopaminergic (TH^+, $GAD67^-$) SN neuron. Two PCR products were detected with agarose gel analysis corresponding to TH (377 bp) and Girk2 (693 bp). *C,* mPCR expression profiling of a single (*wv/wv*) GABAergic (TH^-, $GAD67^+$) SN neuron. Four PCR products were detected with agarose gel analysis corresponding to Girk4 (257 bp), Girk1 (316), Girk2 (693), and GAD67 (702 bp).

sensitive conductance (1.8 ± 0.3 nS; $n = 9$) reversed at −95.9 ± 2.9 mV ($n = 9$; Fig. 8*A,B*) consistent with K-ATP channels. A 100 μM concentration of tolbutamide had no effect on electrical activity or membrane conductances in wild-type DA neurons under metabolic control conditions ($n = 6$; data not shown). We have previously shown that different K-ATP channels are formed in single dopaminergic SN neurons by alternative expression of the sulfonylurea receptor isoforms SUR1 or SUR2B in combination with the pore-forming subunit Kir6.2. This resulted in K-ATP channels with high, intermediate, and low metabolic as well as tolbutamide sensitivities. We also detected that in contrast to wild-type, single (*wv/wv*) dopaminergic SN neurons, exclusively expressed the SUR1 mRNA (Liss et al., 1999). Consistent with these previous findings, *weaver* DA neurons only express K-ATP channels with high tolbutamide sensitivity ($IC_{50} = 6.9 \pm 2.2$ μM; $n = 6$; Fig. 8*C*).

If K-ATP channel activation is a secondary consequence of *wv*Girk2 channel activity, chronic block of *wv*Girk2 channels might reduce metabolic stress and ATP consumption and thus also remove the stimulus for K-ATP channel activation. Therefore, chronic *wv*Girk2 channel inhibition might be permissive for wild-type pacemaker activity in intact neurons that will be able to readjust their metabolism after the inhibition of *wv*Girk2 channels. Indeed, preincubation of midbrain slices for 30 min in 100 μM QX-314 resulted in membrane conductances and electrical pacemaker activity of (*wv/wv*) dopaminergic SN neurons that were not significantly different ($p > 0.05$) from those of wild-type neurons (3.0 ± 1.5 Hz; threshold, −33.8 ± 3.8 mV; AHP, −55.8 ± 3.1 mV; AP, 7.0 ± 1.5 msec; $n = 10$; Fig. 9). This demonstrated that K-ATP channel activation is a specific cellular response of dopaminergic SN neurons to the *gain-of-function* mutation of Girk2. It also indicates that apart from the reversible K-ATP channel activation there are no further secondary changes in ionic conductances in (*wv/wv*) dopaminergic SN neurons.

If the activation of K-ATP channels in response to the *gain-of-function* mutation of Girk2 is a protective cellular response, the SUR1-expressing dopaminergic SN neurons might have a better chance to survive in *weaver*. A cellular marker for dopaminergic SN neurons surviving neurodegeneration, not only in *weaver* but also in Parkinson's disease, is the expression of the calcium-binding protein calbindin D_{28K}. Again we used single-cell RT-mPCR to analyze calbindin expression in wild-type and (*wv/wv*) dopaminergic SN neurons. Although only 15% of single wild-type dopaminergic SN neurons expressed calbindin ($n = 45$), all analyzed (*wv/wv*) dopaminergic SN neurons were calbindin-positive ($n = 6$; Fig. 10). This indicates that we study a dopaminergic population that is likely to survive in adult weaver mice. We also found that all of these calbindin-positive (*wv/wv*) dopaminergic SN neurons, which are characterized by coactivated *wv*Girk2 and K-ATP channels, exclusively express the suphonylurea receptor isoform SUR1 in combination with Kir6.2 (Fig. 10*A*). In contrast, for calbindin-positive wild-type SN neurons we detected alternative SUR expression profiles (Fig. 10*B*) as previously described (Liss et al., 1999). These results indicated that the activity of two membrane conductances, homomeric *wv*Girk2 channels and SUR1/Kir6.2-mediated K-ATP channels, respectively, contribute to the cellular phenotype of calbindin-positive dopaminergic neurons in the *weaver* mouse.

DISCUSSION

Our results demonstrate a *gain-of-function* phenotype in dopaminergic SN neurons in the homozygous *weaver* (*wv/wv*) mouse. In contrast to wild-type (+/+), these *wv/wv* SN neurons have lost their spontaneous pacemaker activity and are tonically depolarized. This electrophysiological *weaver* phenotype in dopaminergic SN neurons is mediated by the coactivation of a QX-314-sensitive and a sulfonylurea-sensitive conductance, which both were not active in wild-type neurons under control conditions. The QX-314-sensitive conductance had a reversal potential of approximately −25 mV, consistent with being carried by nonselective cationic channels. It was also not sensitive to G-protein activation induced by GTPγS dialysis. The properties of this conductance selectively expressed in homozygous *weaver* DA neurons are consistent with being mediated by functionally expressed homomeric *wv*Girk2 channels (Kofuji et al., 1996; Navarro et al., 1996; Slesinger et al., 1997). In addition, native and recombinant *wv*Girk2 channels possessed almost identical QX-314 sensitivities. Our single-cell RT-mPCR data on Girk1–4 expression supported this notion because Girk2 transcripts are not only present

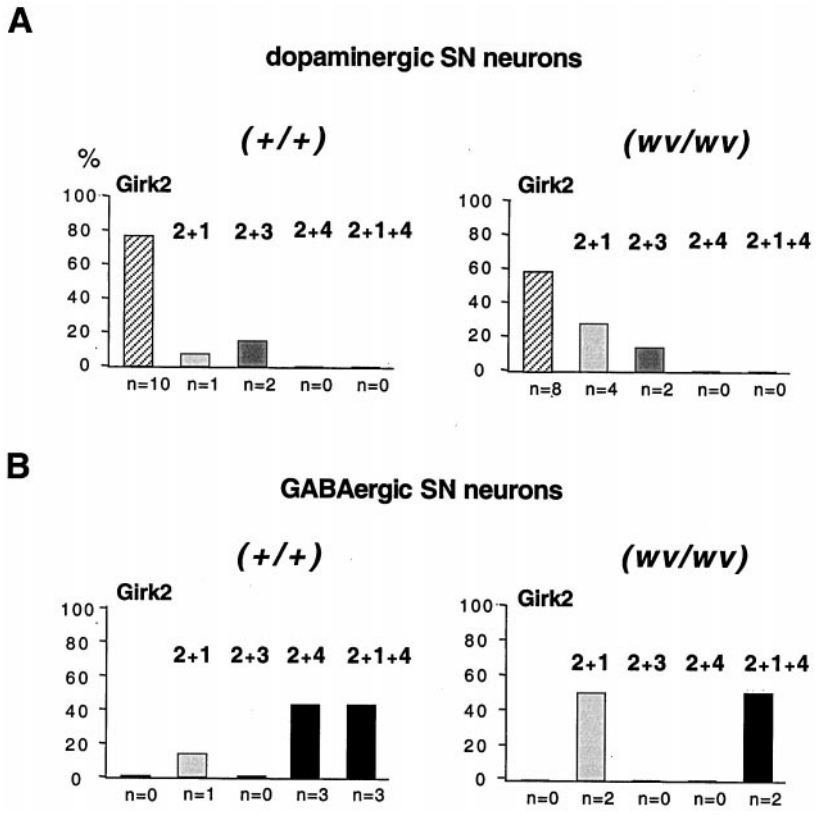

Figure 6. Single-cell coexpression profiles of Girk subunits in (+/+) and (*wv/wv*) dopaminergic (*A*) and GABAergic (*B*) SN neurons. Percentages of Girk1–4 coexpression in single (+/+) and (*wv/wv*) dopaminergic (TH^+) (*A*) and GABAergic ($GAD67^+$) (*B*) SN neurons. Note absence of exclusive Girk2 expression in GABAergic SN neurons.

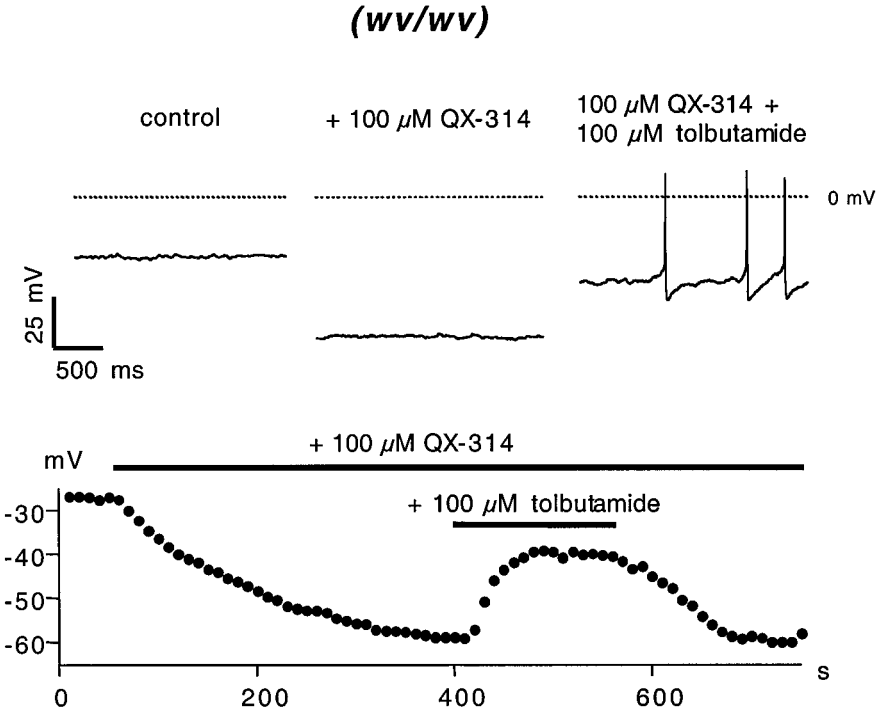

Figure 7. Coactivation of *wv*Girk2 and K-ATP channels determine the phenotype in (*wv/wv*) dopaminergic SN neurons. Standard whole-cell current-clamp recordings of spontaneous electrical activity in a (*wv/wv*) dopaminergic SN neuron. *Top panels* show activity under control, in the presence of 100 μM QX-314, and during coapplication of QX-314 and 100 μM tolbutamide. *Bottom panels* plot the time course of the membrane potential determined in 10 sec intervals during application of QX-314 and tolbutamide as indicated by *bars*. *Dotted lines* indicate zero levels.

in all analyzed dopaminergic SN neurons but in contrast to GABAergic SN neurons, Girk2 is not coexpressed with other Girk family members in the majority of cells. Thus, the formation of homomeric *wv*Girk2 channels is likely to occur in many dopaminergic SN neurons but will be prevented in GABAergic SN neurons. Controlling the number of functional *wv*Girk2 channels may be a crucial mechanism that enables some dopaminergic SN neurons in the *weaver* mouse to avoid a lethal depolarization. In this context, we found no evidence that coexpression of additional Girk family members is a dominant option in dopaminergic SN neurons. In addition, dopaminergic SN neurons coexpressing other Girk family members with Girk2 did not have significantly smaller input conductances. It is important to note that our single-cell RT-PCR protocol does not distinguish between the

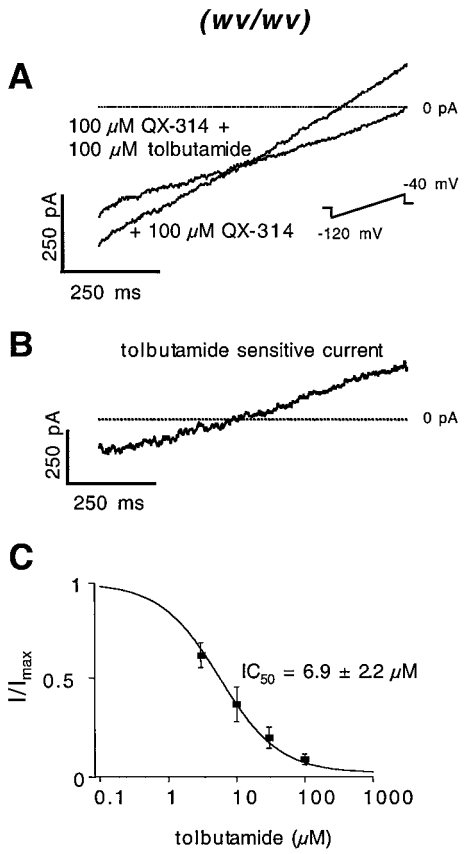

Figure 8. Properties of active K-ATP channels in (*wv/wv*) dopaminergic SN neurons. *A,* Current responses of a (*wv/wv*) dopaminergic SN neuron to voltage ramps from −120 to −40 mV from a holding potential of −60 mV in the presence of 100 μM QX-314 and in 100 μM QX-314 + 100 μM tolbutamide as indicated. *B,* Tolbutamide-sensitive current obtained by subtraction of traces in *A*. *Dotted lines* indicate zero levels. *C,* Dose–response curve for tolbutamide-inhibition of whole-cell currents in (*wv/wv*) dopaminergic SN neurons. *Filled squares* represent means of six separate experiments. *Vertical lines* indicate SEM. The line represents the fit of the mean data by Hill equations with an IC_{50} of 6.9 μM and a Hill coefficient of 0.9.

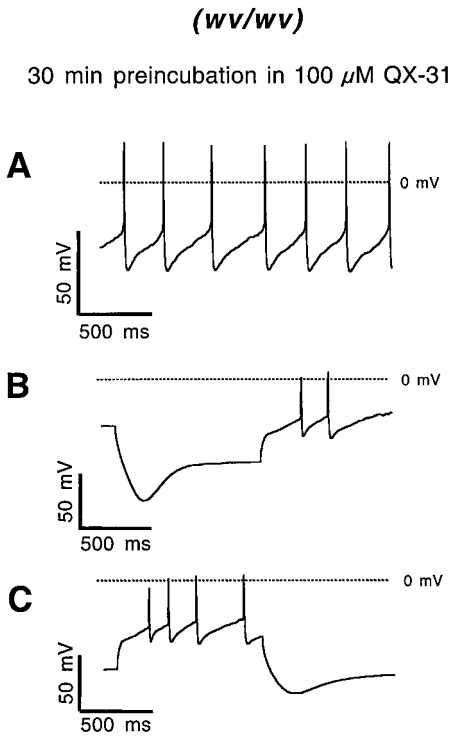

Figure 9. QX-314 preincubation induces wild-type-like electrical properties in (*wv/wv*) dopaminergic SN neurons. Standard whole-cell current-clamp recording of a (*wv/wv*) dopaminergic SN neuron after 30 min preincubation in 100 μM QX-314. *A,* Spontaneous electrical activity; *B,* response of membrane potential to injection of −100 pA hyperpolarizing current; and *C,* responses of membrane potential to injection of +100 pA depolarizing current. *Dotted lines* indicate zero levels.

different Girk2 splice variants and that the results are not quantitative i.e., we have no information on the relative abundance of Girk1 and Girk3 mRNA compared to that of Girk2 in coexpressing dopaminergic SN neurons. Additional mechanisms might be operative both on mRNA and protein levels, e.g., differential expression of Girk2 splice variants (Inanobe et al., 1999, Wei et al., 1998) or Girk channel protein downregulation (Liao et al., 1996), which control the number of homomeric *wv*Girk2 channels. In this context, it is an interesting question how *wv*Girk2 and wild-type Girk2 subunits interact in dopaminergic neurons of heterozygous *weaver* mouse. We demonstrated that dopaminergic SN neurons in heterozygous *weaver* possess slightly different electrophysiological properties compared to wild-type, suggesting that the formation of mutant Girk2 channels might not be fully prevented in these (*wv/+*) neurons. This is consistent with recent reports that demonstrated that a mild form of neurodegeneration of dopaminergic midbrain neurons does also occur in heterozygous *weaver* mice (Verina et al., 1997).

In contrast to conflicting results from cerebellar granule cells (Kofuji et al., 1996; Surmeier et al., 1996; Slesinger et al., 1997; Rossi et al., 1998), we present molecular and functional evidence at the level of single cells that dopaminergic SN neurons clearly possess a *gain-of-function* mutation during the most active stage of neurodegeneration (Verney et al., 1995). *wv*Girk2 channels disturb the physiological activity of dopaminergic neurons. The chronic depolarization might lead to sodium and calcium overload, and consequently to cell death (Kofuji et al., 1996). A novel and surprising aspect of the *weaver* phenotype of dopaminergic SN neurons is our finding that K-ATP channels are coactivated in *weaver* dopaminergic SN neurons and actively contribute to the altered electrophysiological phenotype. Only acute inhibition of both *wv*Girk2 and K-ATP channels reestablished wild-type-like electrical activity, demonstrating the cooperative role of both channel types in determining the *weaver* phenotype. Preincubation of intact (i.e., non-patched) neurons with the *wv*Girk2 blocker QX-314 alone also induced wild-type-like pacemaker activity. This indicated that K-ATP channel activation is induced by active *wv*Girk2 channels in a specific and reversible manner. How might the activity of *wv*Girk2 channels activate K-ATP channels? The *wv*Girk2-mediated sodium load might stimulate Na/K-ATPase activity and thus reduce cytosolic ATP concentrations finally leading to a disinhibition of K-ATP channels. Indeed, recent studies demonstrated that intracellular sodium loading (Seutin et al., 1996) activated K-ATP channels in dopaminergic SN neurons similar to other forms of metabolic stress (Röper and Ashcroft, 1995; Stanford and Lacey, 1995; Watts et al., 1995; Liss et al., 1999). Open K-ATP channels will partially counterbalance the *wv*Girk2-induced membrane depolarization but will also increase the driving force for more sodium entry. As a rise of the intracellular sodium concentration will also directly stimulate

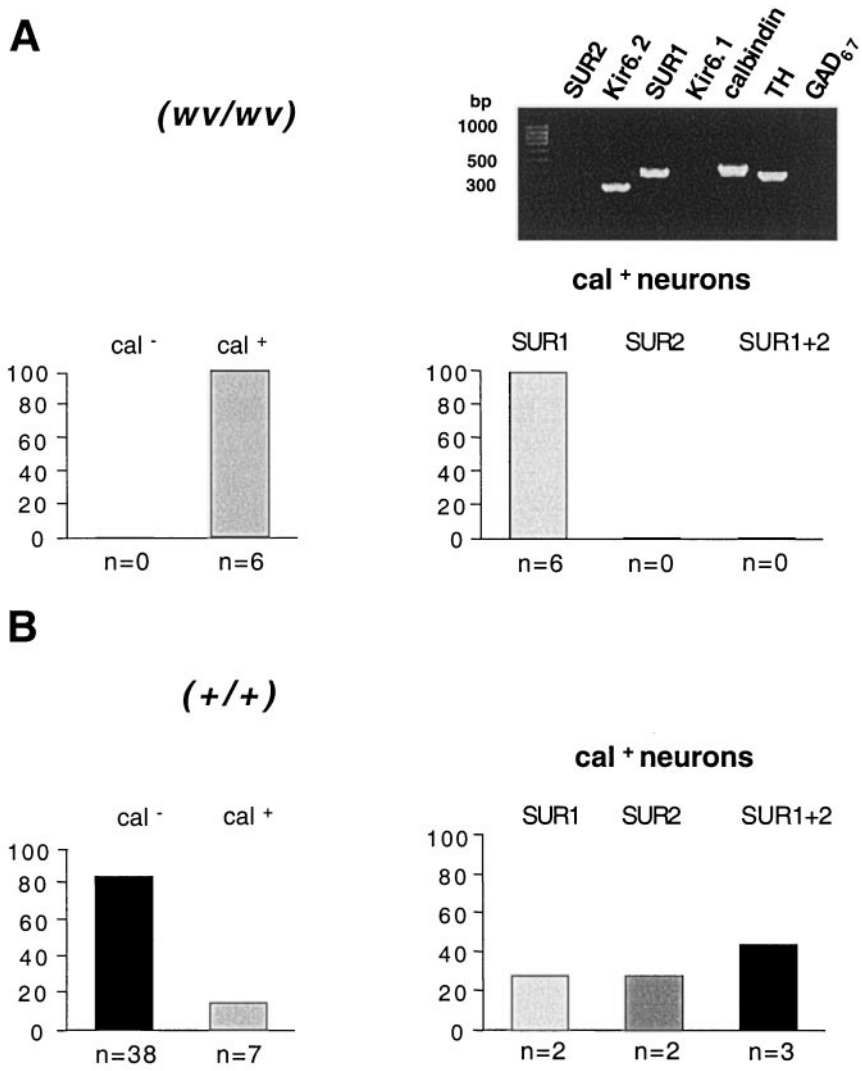

Figure 10. Single-cell calbindin D_{28K} and K-ATP channel subunit expression in (+/+) and (*wv*/*wv*) dopaminergic SN neurons. *Left panels,* Percentages of calbindin-positive and calbindin-negative dopaminergic SN neurons in (*wv*/*wv*) (*A*) and (+/+) (*B*) dopaminergic SN neurons. *Right panels,* Percentages of SUR isoform expression in calbindin-positive and Kir6.2-positive (*wv*/*wv*) (*A*) and (+/+) (*B*) dopaminergic SN neurons. *Insert,* mPCR expression profiling of a single (*wv*/*wv*) dopaminergic (TH^+, $GAD67^-$) SN neuron. Four PCR products were detected with gel analysis corresponding to Kir6.2 (298 bp), SUR1 (401 bp), calbindin (440 bp), and TH (377 bp).

*wv*Girk2 channels activity, *wv*Girk2 and K-ATP channels might be coupled by a positive feedback loop (Silverman et al., 1996).

In addition to the control of *wv*Girk2-mediated channels, the expression of K-ATP channel subunits is also likely to be involved in neuronal survival in the *weaver* mouse. We have recently shown that wild-type dopaminergic SN neurons display a heterogeneous K-ATP subunit profile with alternative expression of the sulfonylurea receptor isoforms SUR1 and SUR2B. We could also demonstrate that alternative SUR expression correlated on the single-cell level with the metabolic sensitivity of K-ATP channels, with SUR1-mediated K-ATP channels possessing a 200-fold higher sensitivity compared to SUR2-mediated channels (Liss et al., 1999). In the same study, we detected a surprisingly homogeneous K-ATP channel expression profile for *weaver* dopaminergic SN neurons. All cells coexpressed only SUR1 + Kir6.2, whereas transcripts of the SUR2 isoform were not detected in (*wv*/*wv*) dopaminergic SN neurons. Here, we described a high sulfonlyurea sensitivity (IC_{50} = 7 μM) in all (*wv*/*wv*) dopaminergic SN neurons consistent with the pharmacological properties of SUR1-containing K-ATP channels. The striking differences in K-ATP channel expression profiles between wild-type and *weaver* might indicate that the expression of SUR1-mediated K-ATP channels does not only contribute to the *weaver* phenotype but is also relevant for selective survival of a subpopulation of (*wv*/*wv*) dopaminergic neurons. The *weaver* mutation does not induce neurodegeneration in all Girk2-expressing DA neurons but targets a highly vulnerable mesostriatal subsystem of DA neurons (Graybiel et al., 1990; Bayer et al., 1995b; Adelbrecht et al., 1997). A similar pattern of subpopulation-selective degeneration within the substantia nigra has been described in idiopathic Parkinson's disease and its neurotoxicological animal models (Hirsch et al., 1997; Lang and Lozano, 1998). The Girk2 mutation defines the initial metabolic stressor in the *weaver* model. A similar role of Girk2 mutations for Parkinson's disease has been excluded (Bandmann et al., 1996). Several other genetic or metabolic candidate trigger mechanisms have been proposed for Parkinson's disease (Hirsch et al., 1997; Lozano et al., 1998). However, the molecular mechanisms of the selective vulnerability of dopaminergic SN neurons in Parkinson's disease remain unresolved. In Parkinson's disease as well as in the *weaver* model, a marker for surviving dopaminergic SN neurons is the presence of the calcium-binding protein calbindin. Our single-cell RT-mPCR experiments showed that in contrast to wild-type all analyzed (*wv*/*wv*) dopaminergic SN neurons were calbindin-positive and thus likely to be members of the most resistant subpopulation of dopaminergic neurons. Thus our data strongly suggest that selective expression and coactivation of SUR1-mediated K-ATP channels with high metabolic sensitivity is relevant for the survival of

dopaminergic SN neurons in the *weaver* mouse. It is possible that selective K-ATP channel expression and activation might also constitute a molecular mechanism involved in the differential vulnerability of dopaminergic SN neurons in Parkinson's disease.

REFERENCES

Adelbrecht C, Murer MG, Lauritzen I, Lesage F, Ladzunski M, Agid Y, Raisman-Vozari R (1997) An immunocytochemical study of a G-protein-gated inward rectifier K+ channel (GIRK2) in the weaver mouse mesencephalon. NeuroReport 8:969–974.

Bandmann O, Davis MB, Marsden CD, Wood NW (1996) The human homologue of the weaver mouse gene in familial and sporadic Parkinson's disease. Neuroscience 72:877–879.

Bayer SA, Wills KV, Triarhou LC, Thomas JD, Ghetti B (1995a) Systematic differences in time of dopaminergic neuron origin between normal mice and homozygous weaver mutants. Exp Brain Res 105:200–208.

Bayer SA, Wills KV, Triarhou LC, Verina T, Thomas JD, Ghetti B (1995b) Selective vulnerability of late-generated dopaminergic neurons of the substantia nigra in weaver mutant mice. Proc Natl Acad Sci USA 92:9137–9140.

Bayer SA, Wills KV, Wei J, Feng Y, Dlouhy SR, Hodes ME, Verina T, Ghetti B (1996) Phenotypic effects of the weaver gene are evident in the embryonic cerebellum but not in the ventral midbrain. Brain Res Dev Brain Res 96:130–137.

Gaspar P, Ben Jelloun N, Febvret A (1994) Sparing of the dopaminergic neurons containing calbindin-D28k and of the dopaminergic mesocortical projections in weaver mutant mice. Neuroscience 61:293–305.

Grace A, Onn S-P (1989) Morphology and electrophysiological properties of immunocytochemically identified rat dopamine neurons recorded in vitro. J. Neurosci 9:3463–3481.

Graybiel AM, Ohta K, Roffler-Tarlov S (1990) Patterns of cell and fiber vulnerability in the mesostriatal system of the mutant mouse weaver. I. Gradients and compartments. J Neurosci 10:720–733.

Heginbotham L, Lu Z, Abramson T, MacKinnon R (1994) Mutations in the K channel signature sequence. Biophys J 66:1061–1067.

Hirsch E, Faucheux B, Damier P, Mouatt-Prigent A, Agid Y (1997) Neuronal vulnerability in Parkinson's disease. J Neural Transm 50:79–88.

Inanobe A, Yoshimoto Y, Horio Y, Morishige KI, Hibino H, Matsumoto S, Tokunaga Y, Maeda T, Hata Y, Takai Y, Kurachi Y (1999) Characterization of G-protein-gated K+ channels composed of Kir3.2 subunits in dopaminergic neurons of the substantia nigra. J Neurosci 19:1006–1017.

Kim KM, Nakajima Y, Nakajima S (1995) G protein-coupled inward rectifier modulated by dopamine agonists in cultured substantia nigra neurons. Neuroscience 69:1145–1158.

Kofuji P, Hofer M, Millen KJ, Millonig JH, Davidson N, Lester HA, Hatten ME (1996) Functional analysis of the weaver mutant GIRK2 K+ channel and rescue of weaver granule cells. Neuron 16:941–952.

Kubisch C, Schroeder BC, Friedrich T, Luetjohann B, El-Amraoui A, Marlin S, Petit C, Jentsch TJ (1999) KCNQ4, a novel potassium channel expressed in sensory outer hair cells, is mutated in dominant deafness. Cell 96:437–446.

Lacey MG, Mercuri NB, North RA (1988) On the potassium conductance increase activated by GABAB and dopamine D2 receptors in rat substantia nigra neurones. J Physiol (Lond) 401:437–453.

Lacey M, Mercuri N, North R (1989) Two cell types in rat substantia nigra zona compacta distinguished by membrane properties and the actions of dopamine and opioids. J Neurosci 9:1233–1241.

Lane PW (1964) New mutation: weaver, wv. Mouse News Letter 30:32–33.

Lang A, Lozano A (1998) Parkinson's disease. N Engl J Med 339:1044–1053.

Liao YJ, Jan YN, Jan LY (1996) Heteromultimerization of G-protein-gated inwardly rectifying K+ channel proteins GIRK1 and GIRK2 and their altered expression in weaver brain. J Neurosci 16:7137–7150.

Liss B, Bruns R, Roeper J (1999) Alternative sulfonylurea receptor expression defines metabolic sensitivity of K-ATP channels in dopaminergic midbrain neurons. EMBO J 18:833–846.

Lozano AM, Lang AE, Hutchison WD, Dostrovsky JO (1998) New developments in understanding the etiology of Parkinson's disease and in its treatment. Curr Opin Neurobiol 8:783–790.

Miki T, Tashiro F, Iwanaga T, Nagashima K, Yoshitomi H, Aihara H, Nitta Y, Gonoi T, Inagaki N, Miyazaki J-I, Seino S (1997) Abnormalities of pancreatic islets by targeted expression of a dominant-negative KATP channel. Proc Natl Acad Sci USA 94:11969–11973.

Navarro B, Kennedy ME, Velimirovic B, Bhat D, Peterson AS, Clapham DE (1996) Nonselective and G $\beta\gamma$-insensitive weaver K+ channels. Science 272:1950–1953.

Nelson E, Liang C, Sinton C, German D (1996) Midbrain dopaminergic neurons in the mouse: computer-assisted mapping. J Comp Neurol 369:361–371.

Patil N, Cox DR, Bhat D, Faham M, Myers RM, Peterson AS (1995) A potassium channel mutation in weaver mice implicates membrane excitability in granule cell differentiation. Nat Genet 11:126–129.

Rakic P, Sidman RL (1973) Sequence of developmental abnormalities leading to granule cell deficit in cerebellar cortex of weaver mutant mice. J Comp Neurol 152:103–132.

Rezai Z, Yoon CH (1972) Abnormal rate of granule cell migration in the cerebellum of "Weaver" mutant mice. Dev Biol 29:17–26.

Richards CTS, Kitai S (1997) Electrophysiological and immunocytochemical characterization of GABA and dopamine neurons in the substantia nigra of the rat. Neuroscience 80:545–557.

Röper J, Ashcroft F (1995) Metabolic inhibition and low internal ATP activate K-ATP channels in rat dopaminergic substantia nigra neurons. Pflügers Arch 430:44–54.

Rossi P, De Filippi G, Armano S, Taglietti V, D'Angelo E (1998) The weaver mutation causes a loss of inward rectifier current regulation in premigratory granule cells of the mouse cerebellum. J Neurosci 18:3537–3547.

Schmidt MJ, Sawyer BD, Perry KW, Fuller RW, Foreman MM, Ghetti B (1982) Dopamine deficiency in the weaver mutant mouse. J Neurosci 2:376–380.

Seutin V, Shen K-Z, North R, Johnson S (1996) Sulphonylurea-sensitive potassium current evoked by sodium-loading in rat midbrain dopamine neurons. Neuroscience 71:709–719.

Signorini S, Liao YJ, Duncan SA, Jan LY, Stoffel M (1997) Normal cerebellar development but susceptibility to seizures in mice lacking G protein-coupled, inwardly rectifying K+ channel GIRK2. Proc Natl Acad Sci USA 94:923–927.

Silverman SK, Kofuji P, Dougherty DA, Davidson N, Lester HA (1996) A regenerative link in the ionic fluxes through the weaver potassium channel underlies the pathophysiology of the mutation. Proc Natl Acad Sci USA 93:15429–15434.

Slesinger PA, Patil N, Liao YJ, Jan YN, Jan LY, Cox DR (1996) Functional effects of the mouse weaver mutation on G protein-gated inwardly rectifying K+ channels. Neuron 16:321–331.

Slesinger PA, Stoffel M, Jan YN, Jan LY (1997) Defective gamma-aminobutyric acid type B receptor-activated inwardly rectifying K+ currents in cerebellar granule cells isolated from weaver and Girk2 null mutant mice. Proc Natl Acad Sci USA 94:12210–12217.

Stanford IM, Lacey MG (1995) Regulation of a potassium conductance in rat midbrain dopamine neurons by intracellular adenosine triphosphate (ATP) and the sulfonylureas tolbutamide and glibenclamide. J Neurosci 15:4651–4657.

Stuart G, Dodt H-U, Sakmann B (1993) Patch-clamp recordings from the soma and dendrites of neurons in brain slices using infrared video microscopy. Pflügers Arch 423:511–518.

Surmeier DJ, Mermelstein PG, Goldowitz D (1996) The weaver mutation of GIRK2 results in a loss of inwardly rectifying K+ current in cerebellar granule cells. Proc Natl Acad Sci USA 93:11191–11195.

Verina T, Norton JA, Sorbel JJ, Triarhou LC, Laferty D, Richter JA, Simon JR, Ghetti B (1997) Atrophy and loss of dopaminergic mesencephalic neurons in heterozygous weaver mice. Exp Brain Res 113:5–12.

Verney C, Febvret-Muzerelle A, Gaspar P (1995) Early postnatal changes of the dopaminergic mesencephalic neurons in the weaver mutant mouse. Brain Res Dev Brain Res 89:115–119.

Watts A, Hicks G, Henderson G (1995) Putative pre-and postsynaptic ATP-sensitive potassium channels in the rat substantia nigra in vitro. J Neurosci 15:3065–3074.

Wei J, Hodes ME, Piva R, Feng Y, Wang Y, Ghetti B, Dlouhy SR (1998) Characterization of murine Girk2 transcript isoforms: structure and differential expression. Genomics 51:379–390.